Published in final edited form as:
Neuropharmacology. 2012 December ; 63(7): 1218–1226. doi:10.1016/j.neuropharm.2012.07.043.

Vasopressin Facilitates GABAergic Transmission in Rat Hippocampus via Activation of V_{1A} receptors

Gunasekaran Ramanathan, **Nicholas I. Cilz**, **Lalitha Kurada**, **Binqi Hu**, **Xiaoping Wang**, and **Saobo Lei***
Department of Pharmacology, Physiology and Therapeutics, School of Medicine and Health Sciences, University of North Dakota, Grand Forks, ND58203, USA

Abstract

Whereas vasopressin has been shown to enhance memory possibly by increasing long-term potentiation and direct excitation of the pyramidal neurons in the hippocampus, the effects of vasopressin on GABAergic transmission in the hippocampus remain to be determined. Here we examined the effects of vasopressin on GABAergic transmission onto CA1 pyramidal neurons and our results demonstrate that bath application of [Arg^8]-vasopressin (AVP) dose-dependently increased the frequency of spontaneous IPSCs (sIPSCs) recorded from CA1 pyramidal neurons via activation of V_{1A} receptors. Immunohistological staining and western blot further confirmed that both CA1 pyramidal neurons and interneurons expressed V_{1A} receptors. Bath application of AVP altered neither the frequency nor the amplitude of miniature IPSCs in the presence of tetradotoxin and failed to change significantly the amplitude of evoked IPSCs recorded from CA1 pyramidal neurons. AVP increased the firing frequency of action potentials by depolarizing the GABAergic interneurons in the stratum radiatum of CA1 region. AVP-mediated depolarization of interneurons was mediated by inhibition of a background K^+ conductance which was insensitive to extracellular tetraethylammonium, Cs^+, 4-aminopyridine, tertiapine-Q and Ba^{2+}. AVP-induced depolarization of interneurons was dependent on $G\alpha_{q/11}$ but independent of phospholipase C, intracellular Ca^{2+} release and protein kinase C. The inhibitory effects of AVP-mediated modulation of GABA release onto CA1 pyramidal neurons were overwhelmed by its strong excitation of CA1 pyramidal neurons in physiological condition but revealed when its direct excitation of the pyramidal neurons was blocked suggesting that AVP-mediated modulation of GABAergic transmission fine-tunes the excitability of CA1 pyramidal neurons.

Keywords

synaptic transmission; K^+ channels; GABA receptor; hippocampus; G-protein; synapse

1. Introduction

The nonapeptide vasopressin is a neurohypophyseal hormone that targets kidney, blood vessels, liver, platelets and anterior pituitary (Raggenbass, 2008). Vasopressin also serves as a neuromodulator in the brain and interacts with three types of receptors: V_{1A}, V_{1B} and V_2

*Correspondence: Saobo Lei Department of Pharmacology, Physiology and Therapeutics, School of Medicine and Health Sciences, University of North Dakota, Grand Forks, ND58203, USA. 701-777-4745 (phone) 701-777-4490 (fax) slei@medicine.nodak.edu.

receptors (Raggenbass, 2008). Both V_{1A} and V_{1B} receptors are coupled to phospholipase C (PLC) which hydrolyzes phosphatidylinositol 4, 5-bisphosphate (PIP_2) into inositol trisphosphate (IP_3) to increase intracellular Ca^{2+} release and diacylglycerol to activate protein kinase C (PKC), whereas V_2 receptors enhances adenylyl cyclase activity resulting in increases in the levels of cyclic AMP and protein kinase A activity (Raggenbass, 2008). The biological effects of vasopressin may be mediated by these vasopressin receptors and intracellular molecules.

Vasopressin fibers of the magnocellular nuclei project to many areas of the central nervous system including the amygdala, hippocampus and spinal cord (Buijs, 1980). The immunoreactivity of vasopressin has been detected in the thalamus, medulla, cerebellum, amygdala, substantia nigra and hippocampus (Hawthorn et al., 1980; Tiberiis et al., 1983b). In addition, the hippocampus also expresses high-density of vasopressin receptors (Audigier and Barberis, 1985; Brinton et al., 1984; Costantini and Pearlmutter, 1984; De Kloet et al., 1985). Consistent with the distribution of vasopressin and vasopressin receptors in the hippocampus, application of vasopressin enhances synaptic transmission and induces long-term potentiation (LTP) in CA1 region (Chepkova et al., 1995; Chepkova et al., 2001; Rong et al., 1993) and the dentate gyrus (Chen et al., 1993; Dubrovsky et al., 2003). Whereas vasopressin has been shown to excite hippocampal pyramidal neurons (Mizuno et al., 1984; Muhlethaler et al., 1982; Tiberiis et al., 1983a), recordings of the field potentials demonstrate that the pyramidal discharge is inhibited by vasopressin (Albeck and Smock, 1988) suggesting that vasopressin also excites non-pyramidal inhibitory interneurons to exert indirect inhibitory effects on pyramidal neurons (Muhlethaler et al., 1984). However, the effects of vasopressin on interneurons and the underlying cellular and molecular mechanisms have not been determined. Because hippocampal interneurons are GABAergic neurons, we probed the effects of vasopressin on GABAergic transmission. Our results demonstrate that vasopressin augments GABAergic transmission onto CA1 pyramidal neurons in the hippocampus.

2. Materials and Methods

2.1. Slice preparation

Horizontal brain slices (400 μm) including the EC, subiculum and hippocampus were cut using a vibrating blade microtome (VT1000S; Leica, Wetzlar, Germany) from 13- to 20-day-old Sprague-Dawley rats as described previously (Deng and Lei, 2006, 2007; Deng et al., 2010; Lei et al., 2007; Xiao et al., 2009a). After being deeply anesthetized with isoflurane, rats were decapitated and their brains were dissected out in ice-cold saline solution that contained (in mM) 130 NaCl, 24 $NaHCO_3$, 3.5 KCl, 1.25 NaH_2PO_4, 0.5 $CaCl_2$, 5.0 $MgCl_2$, and 10 glucose, saturated with 95% O_2 and 5% CO_2 (pH 7.4). Slices were initially incubated in the above solution at 35°C for 40 min for recovery and then kept at room temperature (~23°C) until use. All animal procedures conformed to the guidelines approved by the University of North Dakota Animal Care and Use Committee.

2.2. Recordings of spontaneous, miniature and evoked $GABA_A$ receptor-mediated IPSCs

Whole-cell patch-clamp recordings using a Multiclamp 700B amplifier (Molecular Devices, Sunnyvale, CA) in voltage- or current-clamp mode were made from CA1 pyramidal neurons or interneurons in the stratum radiatum of CA1 region visually identified with infrared video microscopy (Olympus BX51WI) and differential interference contrast optics unless stated otherwise. As described previously (Deng and Lei, 2008; Deng et al., 2006; Wang et al., 2012; Wang et al., 2011; Xiao et al., 2009b), the recording electrodes were filled with (mM) 100 cesium gluconate, 0.6 EGTA, 5 $MgCl_2$, 8 NaCl, 2 ATP_2Na, 0.3 GTPNa, 40 HEPES, and 1 QX-314 (pH 7.3). The extracellular solution comprised (mM) 130 NaCl, 24 $NaHCO_3$,

3.5 KCl, 1.25 NaH_2PO_4, 1.5 $MgCl_2$, 2.5 $CaCl_2$ and 10 glucose, saturated with 95% O_2 and 5% CO_2 (pH 7.4). To record $GABA_A$ receptor-mediated spontaneous IPSCs (sIPSCs), the external solution was supplemented with *dl*-APV (100 μM) to block NMDA and DNQX (10 μM) to block AMPA/kainate receptor-mediated responses, respectively. sIPSCs were recorded at a holding potential of +30 mV. Miniature IPSCs (mIPSCs) were recorded by including TTX (0.5 μM) in the above external solution to block action potential-dependent responses. Evoked IPSCs (eIPSCs) were recorded from CA1 pyramidal neurons using the same internal and external solution by placing a stimulation electrode in the stratum radiatum of CA1 region. Data were filtered at 2 kHz, digitized at 10 kHz and acquired on-line using pCLAMP 9 (Clampex) software (Molecular Devices, Sunnyvale, CA). The recorded sIPSCs and mIPSCs were subsequently analyzed by Mini Analysis 6.0.1 (Synaptosoft Inc., Decatur, GA, USA). Each detected event was inspected visually to exclude obvious artifacts before analysis. Mean amplitude, frequency, cumulative amplitude and frequency histograms were calculated by this program. The recorded eIPSCs were analyzed by pClamp 9 (Clampfit). [Arg^8]-vasopressin (AVP) was applied via the bath. To avoid desensitization induced by repeated applications of AVP, one slice was limited to only one application of AVP.

2.3. Recordings of action potentials (APs)

AP firing was recorded from the interneurons in the stratum radiatum of CA1 region with whole-cell patch-clamp recordings in current-clamp mode as described previously (Deng et al., 2007; Deng et al., 2009). Cs^+-gluconate in the above intracellular solution was replaced with the same concentration of K^+-gluconate and QX-314 was omitted. We waited for ~15 min after the formation of whole-cell configuration to record stable APs. Data were obtained only from those cells displaying resting membrane potential negative to -60 mV. These neurons did not show spontaneous firing and we thus usually injected a positive current to induced AP firing. AVP was applied after the AP firing had been stable for 5~10 min. The frequency of the APs was calculated by Mini Analysis 6.0.1.

2.4. Recording of holding currents (HCs) from GABAergic interneurons

HCs at -60 mV were recorded from the interneurons in the stratum radiatum of CA1 region. The above K^+-containing intracellular solution was used and the extracellular solution contained TTX (0.5 μM) to block potential effects of AVP on synaptic transmission. HCs at -60 mV were recorded every 3 s and then averaged per minute. We subtracted the average of the HCs recorded for the last minute before application of AVP from those recorded at different time points to zero the basal level of the HCs for better comparison. For the experiment involving N-methyl-D-glucamine (NMDG), the extracellular NaCl concentration was replaced by the same concentration of NMDG and HCl was used to adjust pH to 7.4.

2.5. Construction of voltage-current curves

Voltage-current curves were constructed from the interneurons in the stratum radiatum of CA1 region. K^+-gluconate internal solution was used and the extracellular solution was supplemented with (μM) 0.5 TTX, 100 $CdCl_2$, 10 DNQX, 50 *dl*-APV and 10 bicuculline. Voltage-current relationship was obtained by using a ramp protocol from -120 mV to -40 mV at a speed of 0.07 mV/ms. Because the maximal effect of AVP usually occurred at ~5 min, we compared the voltage-current curves recorded before and during the application of AVP for ~5 min.

2.6. Immunocytochemistry

The detailed procedures for immunocytochemistry were described previously (Deng and Lei, 2008; Deng et al., 2009; Xiao et al., 2009a). Briefly, horizontal sections (20 μm) from rat brain were washed in 0.1 M PBS and then treated with 0.3% hydrogen peroxide for 10 min to quench endogenous peroxidase activity. After being rinsed in 0.1 M PBS containing 1% Triton X-100 and 5% normal donkey serum for 30 min, sections were incubated with the primary rabbit anti-rat AVP-V_{1A} IgG (Alpha diagnostic, TX) at a dilution of 1:200 in 1.5% blocking donkey serum in PBS at 4°C for 48 h on a shaker. After wash for 3 times (5 min each) with PBS, sections were incubated for 1 h with biotinylated goat anti-rabbit IgG (Immunocruz™ Staining System, Santa Cruz Biotechnology Inc., CA) followed by incubation for 1 h with HRP-streptavidin complex (Immunocruz™ Staining System). After each incubation, sections were washed three times for a total of 30 min. Diaminobenzidine (Immunocruz™ Staining System) was used for a color reaction to detect the positive signals. We strictly controlled the incubation time to obtain comparable results. Finally, sections were mounted on slides, dehydrated through an alcohol range, cleared in xylene and covered with cover-slips. Slides were visualized and photographed with a Leica microscope (DM 4000B). We stained 5-6 nonadjacent sections and each staining was repeated by using 3 rats.

2.7. Western Blot: Experimental procedures for Western Blot were described previously

(Deng et al., 2009; Xiao et al., 2009a). Briefly, hippocampal tissues for Western Blot experiments were taken from 8 rats (18 days old). For each rat, horizontal brain slices were cut initially, and CA1 region was punched out from the slices under a microscope. The isolated brain region was lysed in tissue protein extraction buffer containing protease inhibitors (Pierce). The lysates were centrifuged at 10,000 x g for 10 min to remove the insoluble materials and protein concentrations in the supernatant were determined (Bradford, 1976). An equivalent of 40 μg of total protein was loaded to each lane. Proteins were separated by 12% SDS-PAGE and transferred to the polyvinylidene difluoride (Immobilon-P, Millipore, Billerica, MA) membranes using an electrophoretic transfer system (Bio-Rad). Blots were blocked with 5% powdered milk, and then incubated with primary rabbit anti-rat AVP-V_{1A} IgG (Alpha diagnostic, TX) at 4°C overnight followed by incubation with the secondary antibody (goat anti-rabbit IgG horseradish peroxidase, 1:2000) for 1 h at room temperature. Tris-buffered saline with 1% Tween 20 was used to wash the blots three times (10 min each) after incubation with both primary and secondary antibodies. Immunoreactive bands were visualized by SuperSignal West Pico Chemiluminescent Substrate (Pierce) and detected by a Biospectrum Imagining System (UVP, Upland, CA).

2.7. Data analysis

Data are presented as the means ± S.E.M. The concentration-response curve of AVP was fit by Hill equation: $I = I_{max} \times \{1/[1 + (EC_{50}/[ligand])^n]\}$, where I_{max} is the maximum response, EC_{50} is the concentration of ligand producing a half-maximal response, and n is the Hill coefficient. Student's paired or unpaired t-test or analysis of variance (ANOVA) was used for statistical analysis as appropriate; *P* values are reported throughout the text and significance was set as $P<0.05$. For sIPSC cumulative probability plots, events recorded for 2 min before AVP application and 2 min of the maximal effect of AVP (usually the third and fourth min from the beginning of AVP application) were selected. Same bin size (25 ms for frequency and 2 pA for amplitude) was used to analyze data from control and AVP treatment. Kolmogorov-Smirnoff test was used to assess the significance of the cumulative probability plots. N number in the text represents the number of cells examined.

2.8. Chemicals

The following reagents were purchased from TOCRIS (Ellisville, MO): GDP-β-S, U73122, calphostin C, Ro-318220, SR49059, SKF96365, tertiapin-Q, tharpsigargin, 2-aminoethyldiphenyl borate (2-APB), CGP55845, bicuculline, 6,7-dinitroquinoxaline-2,3-dione (DNQX) and *dl*-2-amino-5-phosphonopentanic acid (*dl*-APV). [Arg^8]-vasopressin (AVP) was the product of American Peptide Company (Sunnyvale, CA). Anti-$G\alpha_{q/11}$ antibody and control Ig-G were from Enzo Life Sciences (Farmingdale, NY). Other chemicals were products of Sigma-Aldrich (St. Louis, MO).

3. Results

3.1. AVP increases sIPSC frequency recorded from hippocampal CA1 pyramidal neurons

We initially examined the effects of AVP on $GABA_A$ receptor-mediated sIPSCs recorded from CA1 pyramidal neurons. Application of AVP (0.3 μM) for 7 min significantly increased the frequency of sIPSCs to 356±89% of control (Control: 3.1±0.8 Hz, AVP: 8.3±1.4 Hz, n=9, p=0.02, Fig. 1A, 1B, 1C) without altering the amplitude of sIPSCs significantly (99±6% of control; Control: 28.9±2.0 pA, AVP: 28.5±2.4 pA, n=9, p=0.88, Fig. 1A, 1D). The EC_{50} value of AVP was measured to be 41 nM (Fig. 1E). We applied AVP at the concentration of 0.3 μM for the rest of the experiments for better comparison. AVP-induced increases in sIPSC frequency were mediated by V_{1A} receptors because pretreatment of slices with and continuous bath application of SR49059 (1 μM), a selective V_{1A} receptor antagonist, blocked AVP-induced increases in sIPSC frequency (135±26% of control, SR49059: 5.1±2.4 Hz, SR49059+AVP: 5.5±1.8 Hz, n=8, p=0.21, Fig. 1F). Consistent with our electrophysiological results, immunoreactivity of V_{1A} receptors was detected in both pyramidal neurons and interneurons in CA1 region (Fig. 1G). Furthermore, a band of ~43 kDa was detected from the lysates of the CA1 region of the hippocampus by western blot (Fig. 1H), consistent with the reported molecular mass of V_{1A} (Barbeau et al., 1996; Herrera et al., 2008; Kline et al., 2011).

3.2. AVP has no effects on mIPSCs and eIPSCs

Because sIPSCs recorded in the absence of TTX is AP- and Ca^{2+}-dependent, we next examined the effects of AVP on mIPSCs recorded from CA1 pyramidal neurons in the presence of TTX. Bath application of TTX significantly reduced IPSC frequency (Control: 6.9±1.9 Hz, TTX: 2.1±0.8 Hz, n=5, p=0.02, paired t-test) and amplitude (Control: 26.7±4.2 pA, TTX: 22.9±1.3 pA, n=5, p=0.03, paired t-test, data not shown) suggesting that TTX is biologically active. Application of AVP (0.3 μM) changed neither the frequency (99±8% of control, Control: 2.1±0.8 Hz, AVP: 1.9±0.7 Hz, n=5, p=0.95, Fig. 2A, 2B and 2C) nor the amplitude (94±4% of control, Control: 22.9±1.3 pA, AVP: 21.6±0.8 pA, n=5, p=0.22, Fig. 2A, 2D) of mIPSCs suggesting that AVP has no effects on either postsynaptic $GABA_A$ receptors or exocytosis downstream of Ca^{2+} influx. This result also implies that the effects of AVP are AP-dependent. We also examined the effects of AVP on $GABA_A$ receptor-mediated IPSC recorded from CA1 pyramidal neurons evoked by placing a stimulation electrode in the stratum radiatum. Application of AVP (0.3 μM) did not alter significantly the amplitude of eIPSCs (91±6% of control, n=7, p=0.15, Fig. 2E, 2F). Although both sIPSCs and eIPSCs are AP-dependent, the APs underlying eIPSCs are generated by exogenous stimulation-induced depolarization but those responsible for sIPSCs are determined by the intrinsic excitability of neurons. The results that AVP increases sIPSC frequency without altering the eIPSC amplitude suggest that AVP enhances the excitability of GABAergic interneurons to facilitate the generation of APs and GABA release.

3.3. AVP increases the excitability of GABAergic interneurons

We then tested the hypothesis that AVP-mediated increases in sIPSC frequency are due to AVP-induced facilitation of AP generation in GABAergic interneurons resulting in an increase in GABA release. We recorded AP firing from the interneurons in the stratum radiatum of CA1 region because the excitability of pyramidal neurons is subject to the control of interneurons in the stratum radiatum in CA1 region. Application of AVP (0.3 μM) significantly increased the AP firing frequency to 256±25% of control (n=11, $p<0.001$, Fig. 3A and 3B) suggesting that AVP increases GABA release by enhancing the excitability of GABAergic interneurons.

We next tested whether AVP increases AP firing frequency by depolarizing GABAergic interneurons. We recorded AVP-induced changes in resting membrane potentials in current-clamp mode from CA1 stratum radiatum interneurons in the extracellular solution supplemented with TTX (0.5 μM) to block potential indirect effects of AVP on synaptic transmission. A negative current (-50 pA for 500 ms) was injected every 5 s to assess the changes of input resistance induced by AVP (Fig. 3C). Under these circumstances, application of AVP (0.3 μM) generated membrane depolarization (Control: -63.8±1.8 mV, AVP: -58.8±2.6 mV, n=5, p=0.007, Fig. 3C and 3D) and increased input resistance (Control: 492±57 M , AVP: 618±73 MΩ, n=5, p=0.005, Fig. 3C and 3D) suggesting that AVP reduces membrane conductance.

We then recorded the HCs at -60 mV from the interneurons in the stratum radiatum of CA1 region. Application of AVP (0.3 μM) generated an inward HC (-19.3±2.6 pA, n=19, $p<0.001$, Fig. 3E). AVP-induced membrane depolarization was mediated by activation of V_{1A} receptors because pretreatment of slices with and continuous bath application of SR49059 (1 μM), a selective V_{1A} receptor antagonist, blocked AVP-induced increases in inward currents (-3.3±1.8 pA, n=8, p=0.11, Fig. 3F).

3.4. Involvement of background K^+ channels

AVP-induced membrane depolarization could be produced by depression of a background K^+ channel or opening of a cationic channel. We first tested whether AVP-induced depolarization of CA1 interneurons was mediated by inhibition of a background K^+ conductance. Substitution of intracellular K^+ with Cs^+ blocked AVP-induced increases in inward HCs (-1.99±1.14 pA, n=8, p=0.125, Fig. 4A) suggesting that the depolarizing effect of AVP is mediated by inhibition of K^+ channels. We further measured the reversal potential of the net current induced by AVP on the rationale that AVP-induced net current should have a reversal potential close to the K^+ reversal potential if K^+ channels are involved. We used a ramp protocol (from -120 mV to -40 mV, at a speed of 0.07 mV/ms) to construct the voltage-current curve before and during the application of AVP. The intracellular solution contained 100 mM K^+-gluconate and the extracellular solution was supplemented with (in μM) 0.5 TTX, 100 Cd^{2+}, 10 DNQX, 50 *dl*-APV and 10 bicuculline to block synaptic currents and other voltage-gated ion channels. In this condition, application of AVP induced a current which had a reversal potential of -83.8±1.8 mV (n=5) which was close to the calculated K^+ reversal potential (-85.4 mV) when the extracellular K^+ concentration was 3.5 mM (Fig. 4B). When the extracellular K^+ concentration was elevated to 10 mM, the reversal potential of AVP-induced net currents shifted to -61.7±1.9 mV (n=6, Fig. 4C) which is close to the calculated K^+-reversal potential (-58.7 mV) under these circumstances. These results suggest that AVP induces membrane depolarization by inhibiting K^+ channels responsible for controlling the resting membrane potentials.

Whereas the above results indicate the involvement of a background K^+ channel in AVP-induced depolarization of GABAergic interneurons, we still examined whether cationic

channels play a role. If AVP opens a cationic conductance, the influx of extracellular Na^+ and/or Ca^{2+} should be the major ions to generate the inward currents. We therefore replaced NaCl in the extracellular solution with the same concentration of NMDG-Cl. In this condition, application of AVP (0.3 μM) still induced a comparable inward holding current (-17.9±3.1 pA, n=8, p=0.001, Fig. 4D). Furthermore, deprivation of Ca^{2+} from the extracellular solution did not prevent AVP-induced membrane depolarization (-14.8±2.0 pA, n=15, p<0.001, Fig. 4E). Finally, we used cationic channel blockers and tested the roles of cationic channels in AVP-induced depolarization of interneurons. AVP-induced increases in inward HCs were not significantly altered (vs. AVP alone, Fig. 4F) in the presence of Gd^{3+} (10 μM, n=11, p=0.57), La^{3+} (10 μM, n=7, p=0.6) and SKF96365 (100 μM, n=7, p=0.29). Taken together, we concluded that AVP-induced membrane depolarization in interneurons is unlikely related to the opening of a cationic conductance.

We next characterized the properties of the involved K^+ channels. AVP-induced increases in inward HCs recorded from interneurons in the stratum radiatum of CA1 region were not significantly altered (vs. AVP alone, Fig. 4F) when the extracellular solution contained tetraethylammonium (TEA, 10 mM, n=9, p=0.84), Cs^+ (3 mM, n=8, p=0.89) or 4-aminopyridine (4-AP, 2 mM, n=8, p=0.85). Furthermore, inclusion of the specific inward rectifier K^+ channel inhibitor, tertiapin-Q (50 nM), in the extracellular solution did not significantly change AVP-induced increases in inward HCs (n=8, p=0.4 vs. AVP alone, Fig. 4F) suggesting that inward rectifier K^+ channels are unlikely to be involved in AVP-induced depolarization of hippocampal interneurons. Because the two pore-domain K^+ channels (K_{2P}) are involved in controlling resting membrane potentials and they are insensitive to the classical K^+ channel blockers (TEA, 4-AP, Cs^+), the above results suggest the involvement of K_{2P} channels in AVP-induced membrane depolarization in GABAergic interneurons. The family of K_{2P} channels includes TWIK, THIK, TREK, TASK, TALK and TRESK (Bayliss et al., 2003; Lesage, 2003), some of which are sensitive to Ba^{2+}. We therefore tested the role of Ba^{2+} in AVP-induced membrane depolarization. Application of Ba^{2+} (3 mM) alone induced an inward HC (-21.6±8.6 pA, n=8, p=0.04, Fig. 4G) by itself suggesting that Ba^{2+}-sensitive K^+ channels have a significant role in controlling resting membrane potentials. However, AVP-induced increases in inward HCs were not significantly changed in the presence of Ba^{2+} (-15.8±3.5 pA, n=8, p=0.47 vs. AVP alone, unpaired t-test, Fig. 4G) suggesting that the involved K_{2P} channels are not sensitive to Ba^{2+}.

3.5. Signaling mechanisms underlying AVP-induced depolarization of interneurons

Because V_{1A} receptors are G protein-coupled, we tested the roles of G proteins in AVP-mediated depolarization of interneurons. We included the G protein inactivator, GDP-β-S (2 mM), in the recording pipettes and waited for >20 min after the formation of whole-cell configuration to allow the dialysis of GDP-β-S into cells. Intracellular application of GDP-β-S via the recording pipettes completely blocked AVP-induced depolarization (-3.5±4.7 pA, n=8, p=0.48, Fig. 5A) demonstrating the requirement of G proteins. We then tested the roles of PLC by using the selective PLC inhibitor, U73122. Slices were pretreated with U73122 at 10 Mμ for ~ 2 hour and the extracellular solution contained the same concentration of these drugs. Under this condition, AVP-induced increases in inward HCs were not significantly changed (control: -19.3±2.6 pA, n=19 vs. U73122: -22.1±3.0 pA, n=9, p=0.54, unpaired t-test, Fig. 5B) suggesting that the function of PLC is not required for AVP-induced depolarization of interneurons. We also tested the roles of the two downstream targets of PLC, IP_3 receptors and PKC, in AVP-induced depolarization. Slices were pretreated with the IP_3 receptor inhibitors, 2-aminoethyldiphenyl borate (2-APB, 100 μM), and the same concentration of 2-APB was continuously bath-applied in the extracellular solution. In this condition, bath application of AVP (0.3 μM) still induced a comparable inward HCs (-17.7±2.9 pA, n=5, p=0.82 vs. control, unpaired t-test, Fig. 5C)

suggesting that IP_3 receptors are not involved in AVP-mediated depolarization of interneurons. We further tested whether intracellular Ca^{2+} released from other stores is required for AVP-induced increases in inward HCs. Intracellular application of thapsigargin (10 μM) via the recording pipettes to deplete intracellular Ca^{2+} store did not significantly change AVP-induced increases in inward HCs (-19.9±3.5 pA, n=11, p=0.77 vs. control, unpaired t-test, Fig. 5C) further confirming that intracellular Ca^{2+} release is unnecessary for AVP-mediated augmentation of inward HCs. We further dialyzed BAPTA into the cells to chelate intracellular Ca^{2+}. Intracellular dialysis of BAPTA (10 mM) via the recording pipettes for >20 min failed to alter AVP-induced increases in inward HCs (-19.9±4.2 pA, n=6, p=0.91 vs. control, unpaired t-test, Fig. 5D) suggesting that AVP-induced depolarization does not rely on increases in intracellular Ca^{2+} concentration. We finally tested the roles of PKC in AVP-mediated depolarization. Slices were pretreated with the selective PKC inhibitors, calphostin C (1 μM) and the same concentration of calphostin C was continuously bath-applied. In this condition, bath application of AVP (0.3 μM) still induced an inward HC (-26.5±4.9 pA, n=7, Fig. 5E) statistically indistinguishable from control (p=0.19, unpaired t-test). Furthermore, application of AVP to slices treated in the same fashion with another PKC inhibitor, Ro-318220 (1 μM) still increased the inward HCs (-30.3±6.7 pA, n=5, p=0.011, Fig. 5E). These data together suggest that the function of PKC is not required for AVP-induced depolarization of interneurons.

We then examined the roles of $G\alpha_{q/11}$ by intracellular perfusion of anti-$G\alpha_{q/11}$ antibody via the recording pipettes. Intracellular application of anti-$G\alpha_{q/11}$ antibody has been shown to block the signal transduction of a variety of G protein-coupled receptors (Bannister et al., 2002; Deng and Lei, 2008; Deng et al., 2006; Zeng et al., 1996). Intracellular application of anti-$G\alpha_{q/11}$ (20 μg/ml) significantly reduced AVP-mediated increases in inward HCs (-2.8±0.4 pA, n=8) compared with those recorded when control Ig-G was included in the recording pipettes (-24.7±5.3 pA, n=7, p=0.001, Two-way ANOVA, Fig. 5F) suggesting that $G\alpha_{q/11}$ is required for AVP-mediated depolarization of interneurons.

3.6. Effects of AVP-induced increases in GABA release on the excitability of CA1 pyramidal neurons

We next examined the effects of AVP-induced facilitation of GABA release on the excitability of CA1 pyramidal neurons by recording AP firing from these neurons. Because AVP has been shown to increase the excitability of pyramidal neurons (Mizuno et al., 1984; Muhlethaler et al., 1982; Tiberiis et al., 1983a), we tested the effects of AVP-mediated increases in GABA release in different conditions. We first tested the net effects of AVP on the excitability of CA1 pyramidal neurons by including DNQX (10 μM), *dl*-APV (100 μM), bicuculline (10 μM) and CGP55845 (2 μM) in the extracellular solution to block the influence arisen from the indirect effects of AVP on glutamatergic and GABAergic transmission. In this condition, bath application of AVP (0.3 μM) significantly increased the firing frequency of APs (372±30% of control, n=8, p<0.001, Fig. $6A_1$-$6A_2$) whereas application of the V_{1A} receptor antagonist, SR49059 (1 μM) blocked AVP-induced increases in AP firing frequency (111±5% of control, n=5, p=0.113, data not shown) demonstrating that activation of V_{1A} receptors on CA1 pyramidal neurons facilitates the excitability of these neurons. This is also consistent with above results showing that CA1 pyramidal neurons expressed high density of V_{1A} receptors (Fig. 1G). Because V_{1A} receptors are G protein-coupled, we included the G protein inactivator GDP-β-S in the recording pipettes to obviate the effects of AVP on pyramidal neurons. Inclusion of GDP-β-S (2 mM) in the recording pipettes blocked AVP-induced increases in AP firing frequency (104±7% of control, n=8, p=0.56, Fig. $6B_1$-$6B_2$). To isolate the pure effects of AVP-induced increases in GABA release on the excitability of pyramidal neurons, we included GDP-β-S (2 mM) in the recording pipettes and DNQX (10 μM) and *dl*-APV (100 μM) in the

extracellular solution to block glutamatergic transmission. Under these circumstances, bath application of AVP (0.3 μM) significantly reduced AP firing frequency (30±9% of control, n=7, $p<0.001$, Fig. $6C_1$-$6C_2$) demonstrating that AVP-induced increases in GABA release down-regulates the excitability of pyramidal neurons in CA1 region of the hippocampus. However, in physiological condition AVP interacts with both pyramidal neurons and interneurons. We therefore examined the effects of AVP on the excitability of pyramidal neurons in normal extracellular and intracellular solution. In this recording condition, bath application of AVP (0.3 μM) still significantly increased the firing frequency of APs (230±38% of control, n=7, $p<0.001$, Fig. $6D_1$-$6D_2$). However, the percentage of AVP-induced increases in AP firing frequency in the normal extracellular and intracellular solution (Fig. $6D_1$-$6D_2$, 230±38% of control, n=7) was significantly smaller than that in the extracellular solution containing the blockers for synaptic transmission (Fig. $6A_1$-$6A_2$, 372±30% of control, n=8, p=0.04, Two-way ANOVA) suggesting that the decreases in AP firing frequency mediated by AVP-induced increases in GABA release are overwhelmed by AVP-induced direct facilitation of the excitability of CA1 pyramidal neurons.

4. Discussion

Our results demonstrate that AVP increases the frequency without effects on the amplitude of sIPSCs recorded from CA1 pyramidal neurons in the hippocampus via activation of V_{1A} receptors. AVP exerts no effects on the frequency and amplitude of mIPSCs recorded in the presence of TTX suggesting that AVP-induced facilitation of GABAergic transmission is AP-dependent. Activation of V_{1A} receptors facilitates GABAergic transmission by inhibiting a type of background K^+ channels that are insensitive to Ba^{2+}, resulting in membrane depolarization and increases in AP firing frequency of GABAergic interneurons in the hippocampus. AVP-mediated modulation of GABAergic transmission depends on $G\alpha_{q/11}$, but is independent of PLC, intracellular Ca^{2+} and PKC. Furthermore, AVP facilitates the excitability of CA1 pyramidal neurons in the absence of glutamatergic and GABAergic functions via activation of V_{1A} receptors on CA1 pyramidal neurons. The inhibitory effect of AVP-induced GABA release onto CA1 pyramidal neurons was revealed after blockade of its excitatory action on CA1 pyramidal neurons. In physiological condition, the effects of AVP-mediated modulation of GABAergic transmission onto CA1 pyramidal neurons are overwhelmed by its strong facilitation of the excitability of CA1 pyramidal neurons suggesting that AVP-mediated modulation of GABAergic transmission plays a fine tune of the excitability of CA1 pyramidal neurons.

One mechanism whereby AVP augments GABAergic transmission onto CA1 pyramidal neurons is that AVP activates a cationic conductance of GABAergic interneurons. AVP has been shown to activate cationic channels (Bisetti et al., 2006; Raggenbass et al., 1991; Reymond-Marron et al., 2006; Wrobel et al., 2011). However, the following results do not support a role of cationic channels in AVP-mediated modulation of GABA release. First, if cationic channels are involved, inclusion of Cs^+-gluconate in the recording pipettes should not block AVP-induced increases in inward HCs. However, our results demonstrated that replacement of intracellular K^+ with Cs^+ blocked AVP-induced increases in inward HCs. Second, the reversal potential of AVP-induced net current is not close to the reversal potential mediated by cations. Third, if cationic channels are involved, extracellular Na^+ and Ca^{2+} should be the major ions mediating the inward HCs. However, replacement of extracellular Na^+ with NMDG or omission of extracellular Ca^{2+} failed to alter AVP-induced increases in inward HCs. Fourth, inclusion of cationic channel blockers, SKF96365, Gd^{2+} and La^{3+} in the extracellular solution did not have significant effects on AVP-mediated increases in inward HCs. Finally, if cationic channels are involved, AVP should also modulate mIPSCs recorded in the presence of TTX because cationic channels should still functional in the presence of TTX and Ca^{2+} influx through the cationic channels should have

still increased the frequency of mIPSCs. However, we failed to observe any effects of AVP on mIPSCs recorded in the presence of TTX.

Resting K^+ channels are the major determinants of neuronal membrane potential and their inhibition is one of the principal mechanisms by which neurotransmitters or neuromodulators modify neuronal excitability. Our results indicate that AVP modulates GABA release by inhibiting a resting K^+ conductance in CA1 interneurons based on the following lines of evidence. First, AVP increased the input resistance of GABAergic interneurons suggesting that AVP inhibits a membrane conductance. Second, replacement of K^+-gluconate with Cs^+-gluconate blocked AVP-induced increases in inward HCs. Third, the reversal potential of AVP-induced net currents was close to K^+ reversal potential and alterations of extracellular K^+ concentration shifted the reversal potential of the net currents.

Whereas our results have demonstrated that AVP modulates GABAergic transmission onto CA1 pyramidal neurons via inhibition of background K^+ channels, the type of the K^+ channels have not been identified. However, our results demonstrate that the involved K^+ channels are insensitive to the classical K^+ channel blockers such as TEA, extracellular Cs^+ and 4-AP suggesting the involvement of K_{2P} channels. In mammals, seventeen K_{2P} channel genes have been identified, and their mRNA transcripts are expressed in many different cell types and tissues. K_{2P} channels have properties of background or leak K^+ channels, and therefore play a crucial role in setting the resting membrane potential and regulating cell excitability. K_{2P} channels can be grouped according to sequence and functional similarities into 6 subfamilies: TWIK, THIK, TREK, TASK, TALK and TRESK (Bayliss et al., 2003; Lesage, 2003). Among these channels, TASK-1, TASK-3, TREK-1, TREK-2, and TWIK-1 have been reported to be sensitive to Ba^{2+} (Fink et al., 1996; Han et al., 2002; Kim et al., 2000; Lesage et al., 1996). Because our results have shown that the effects of AVP are insensitive to Ba^{2+}, it is reasonable to postulate that AVP may not interact with these K_{2P} channels. Because the hippocampus expresses almost all the K_{2P} channels (Talley et al., 2001) and those K_{2P} channels are likely to assemble as heterogeneous channels, the exact nature of the K_{2P} channels inhibited by AVP remains to be determined only after the molecular identities of these K_{2P} channels in native interneurons are fully elucidated.

Our results indicate that the effects of AVP on GABA release in the hippocampus are mediated by V_{1A} receptors because application of SR49059 blocked AVP-induced increases in both inward HCs and sIPSC frequency. We further showed that activation of the V_{1A} receptors on CA1 pyramidal neurons also increases the excitability of these neurons. Consistent with our electrophysiological results, immunohistological staining demonstrates that both the pyramidal neurons and interneurons in the CA1 region express V_{1A} receptors. V_{1A} receptors are G protein-coupled. Our results have demonstrated that the function of G proteins is required for AVP-mediated increase in GABA releases. However, our results do not support any roles of the intracellular molecules downstream of G-proteins in AVP-mediated increase in GABA release. The major intracellular pathway coupled to V_{1A} receptors is PLC pathway resulting in increases in intracellular Ca^{2+} release and the activation of PKC. However, our results indicate that this pathway is unlikely to be involved. We therefore suggest that V_{1A} receptor activation releases $G\alpha_{q/11}$ which directly interacts with K^+ channels to increase GABA release. Consistent with our results, a direct coupling of $G\alpha_q$ with K_{2P} channels in a mammalian heterologous expression system has been observed (Chen et al., 2006).

In addition to transiently increasing GABAergic transmission, our results also demonstrate that AVP persistently enhance the excitability of CA1 pyramidal neurons in the hippocampus. Because AVP-mediated facilitation of the excitability of pyramidal neurons in the CA1 region was observed in the presence of blockers for both glutamatergic and

GABAergic transmission, the action site of the AVP is likely to be on CA1 pyramidal neurons themselves. In line with our results, previous work has also shown that AVP excites hippocampal pyramidal neurons (Mizuno et al., 1984; Muhlethaler et al., 1982; Tiberiis et al., 1983a). Furthermore, AVP has been shown to increase LTP in CA1 region (Chepkova et al., 1995; Chepkova et al., 2001; Rong et al., 1993) and the dentate gyrus (Chen et al., 1993; Dubrovsky et al., 2003). AVP-mediated direct excitation of CA1 pyramidal neurons and indirect augmentation of glutamatergic transmission onto CA1 pyramidal neurons likely contribute to AVP-induced enhancement of learning and memory (Alescio-Lautier et al., 2000; Alescio-Lautier and Soumireu-Mourat, 1998). If so, what are the physiological functions of AVP-induced transient increases in GABAergic transmission? Because AVP-mediated facilitation of GABAergic transmission onto the CA1 pyramidal neurons is overwhelmed by its powerful excitation of pyramidal neurons in normal physiological condition, it can be speculated that AVP-mediated increases in GABA release may play a fine tune on the excitation of pyramidal neurons and its ultimate action on memory. Moreover, GABAergic interneurons are involved in generating and governing oscillatory activities (Somogyi and Klausberger, 2005) which further orchestrate memory consolidation (Molle and Born, 2011). It is therefore reasonable to speculate that AVP-mediated facilitation of GABA release would play a role in the modulation of learning and memory processes.

5. Conclusions

Our results demonstrate that AVP facilitates GABAergic transmission onto CA1 pyramidal neurons via activation of V_{1A} receptors on GABAergic interneurons. Activation of V_{1A} receptors in interneurons generates membrane depolarization resulting in increases in AP firing frequency via inhibition of a Ba^{2+}-insensitive background K^+ channel. AVP-mediated facilitation of GABAergic transmission is dependent on $G\alpha_{q/11}$ but independent of PLC, intracellular Ca^{2+} and PKC suggesting a direct coupling of $G\alpha_{q/11}$ and background K^+ channels. AVP-mediated facilitation of GABAergic transmission may play a fine tune on the excitability of CA1 pyramidal neurons.

Acknowledgments

This work was supported by National Institutes of Mental Health (MH082881 to S.L.)

References

Albeck D, Smock T. A mechanism for vasopressin action in the hippocampus. Brain Res. 1988; 463:394–397. [PubMed: 3196928]

Alescio-Lautier B, Paban V, Soumireu-Mourat B. Neuromodulation of memory in the hippocampus by vasopressin. Eur J Pharmacol. 2000; 405:63–72. [PubMed: 11033315]

Alescio-Lautier B, Soumireu-Mourat B. Role of vasopressin in learning and memory in the hippocampus. Prog Brain Res. 1998; 119:501–521. [PubMed: 10074809]

Audigier S, Barberis C. Pharmacological characterization of two specific binding sites for neurohypophyseal hormones in hippocampal synaptic plasma membranes of the rat. EMBO J. 1985; 4:1407–1412. [PubMed: 2992930]

Bannister RA, Melliti K, Adams BA. Reconstituted slow muscarinic inhibition of neuronal (Ca(v)1.2c) L-type Ca2+ channels. Biophys J. 2002; 83:3256–3267. [PubMed: 12496094]

Barbeau D, Bouley R, Escher E. Molecular weight determination of the hepatic vasopressin receptor with a high-affinity photoprobe. Int J Pept Protein Res. 1996; 48:364–373. [PubMed: 8919057]

Bayliss DA, Sirois JE, Talley EM. The TASK family: two-pore domain background K+ channels. Mol Interv. 2003; 3:205–219. [PubMed: 14993448]

Bisetti A, Cvetkovic V, Serafin M, Bayer L, Machard D, Jones BE, Muhlethaler M. Excitatory action of hypocretin/orexin on neurons of the central medial amygdala. Neuroscience. 2006; 142:999–1004. [PubMed: 16996221]

Bradford MM. A rapid and sensitive method for the quantitation of microgram quantities of protein utilizing the principle of protein-dye binding. Anal Biochem. 1976; 72:248–254. [PubMed: 942051]

Brinton RE, Gee KW, Wamsley JK, Davis TP, Yamamura HI. Regional distribution of putative vasopressin receptors in rat brain and pituitary by quantitative autoradiography. Proc Natl Acad Sci U S A. 1984; 81:7248–7252. [PubMed: 6095279]

Buijs RM. Immunocytochemical demonstration of vasopressin and oxytocin in the rat brain by light and electron microscopy. J Histochem Cytochem. 1980; 28:357–360. [PubMed: 6989899]

Chen C, Diaz Brinton RD, Shors TJ, Thompson RF. Vasopressin induction of long-lasting potentiation of synaptic transmission in the dentate gyrus. Hippocampus. 1993; 3:193–203. [PubMed: 8394770]

Chen X, Talley EM, Patel N, Gomis A, McIntire WE, Dong B, Viana F, Garrison JC, Bayliss DA. Inhibition of a background potassium channel by Gq protein alpha-subunits. Proc Natl Acad Sci U S A. 2006; 103:3422–3427. [PubMed: 16492788]

Chepkova AN, French P, De Wied D, Ontskul AH, Ramakers GM, Skrebitski VG, Gispen WH, Urban IJ. Long-lasting enhancement of synaptic excitability of CA1/subiculum neurons of the rat ventral hippocampus by vasopressin and vasopressin(4-8). Brain Res. 1995; 701:255–266. [PubMed: 8925289]

Chepkova AN, Kapai NA, Skrebitskii VG. Arginine vasopressin fragment AVP(4-9)facilitates induction of long-term potentiation in the hippocampus. Bull Exp Biol Med. 2001; 131:136–138. [PubMed: 11391395]

Costantini MG, Pearlmutter AF. Properties of the specific binding site for arginine vasopressin in rat hippocampal synaptic membranes. J Biol Chem. 1984; 259:11739–11745. [PubMed: 6480583]

De Kloet ER, Rotteveel F, Voorhuis TA, Terlou M. Topography of binding sites for neurohypophyseal hormones in rat brain. Eur J Pharmacol. 1985; 110:113–119. [PubMed: 2988976]

Deng PY, Lei S. Bidirectional modulation of GABAergic transmission by cholecystokinin in hippocampal dentate gyrus granule cells of juvenile rats. J Physiol. 2006; 572:425–442. [PubMed: 16455686]

Deng PY, Lei S. Long-term depression in identified stellate neurons of juvenile rat entorhinal cortex. J Neurophysiol. 2007; 97:727–737. [PubMed: 17135466]

Deng PY, Lei S. Serotonin increases GABA release in rat entorhinal cortex by inhibiting interneuron TASK-3 K+ channels. Mol Cell Neurosci. 2008; 39:273–284. [PubMed: 18687403]

Deng PY, Porter JE, Shin HS, Lei S. Thyrotropin-releasing hormone increases GABA release in rat hippocampus. J Physiol. 2006; 577:497–511. [PubMed: 16990402]

Deng PY, Poudel SK, Rojanathammanee L, Porter JE, Lei S. Serotonin inhibits neuronal excitability by activating two-pore domain k+ channels in the entorhinal cortex. Mol Pharmacol. 2007; 72:208–218. [PubMed: 17452494]

Deng PY, Xiao Z, Jha A, Ramonet D, Matsui T, Leitges M, Shin HS, Porter JE, Geiger JD, Lei S. Cholecystokinin facilitates glutamate release by increasing the number of readily releasable vesicles and releasing probability. J Neurosci. 2010; 30:5136–5148. [PubMed: 20392936]

Deng PY, Xiao Z, Yang C, Rojanathammanee L, Grisanti L, Watt J, Geiger JD, Liu R, Porter JE, Lei S. GABA(B) receptor activation inhibits neuronal excitability and spatial learning in the entorhinal cortex by activating TREK-2 K+ channels. Neuron. 2009; 63:230–243. [PubMed: 19640481]

Dubrovsky B, Tatarinov A, Gijsbers K, Harris J, Tsiodras A. Effects of arginine vasopressin (AVP) on long-term potentiation in intact anesthetized rats. Brain Res Bull. 2003; 59:467–472. [PubMed: 12576144]

Fink M, Duprat F, Lesage F, Reyes R, Romey G, Heurteaux C, Lazdunski M. Cloning, functional expression and brain localization of a novel unconventional outward rectifier K+ channel. EMBO J. 1996; 15:6854–6862. [PubMed: 9003761]

Han J, Truell J, Gnatenco C, Kim D. Characterization of four types of background potassium channels in rat cerebellar granule neurons. J Physiol. 2002; 542:431–444. [PubMed: 12122143]

Hawthorn J, Ang VT, Jenkins JS. Localization of vasopressin in the rat brain. Brain Res. 1980; 197:75–81. [PubMed: 7397564]

Herrera VL, Bagamasbad P, Didishvili T, Decano JL, Ruiz-Opazo N. Overlapping genes in Nalp6/PYPAF5 locus encode two V2-type vasopressin isoreceptors: angiotensin-vasopressin receptor (AVR) and non-AVR. Physiol Genomics. 2008; 34:65–77. [PubMed: 18413781]

Kim Y, Bang H, Kim D. TASK-3, a new member of the tandem pore K(+) channel family. J Biol Chem. 2000; 275:9340–9347. [PubMed: 10734076]

Kline RJ, O'Connell LA, Hofmann HA, Holt GJ, Khan IA. The distribution of an AVT V1a receptor in the brain of a sex changing fish, Epinephelus adscensionis. J Chem Neuroanat. 2011; 42:72–88. [PubMed: 21723386]

Lei S, Deng PY, Porter JE, Shin HS. Adrenergic facilitation of GABAergic transmission in rat entorhinal cortex. J Neurophysiol. 2007; 98:2868–2877. [PubMed: 17804573]

Lesage F. Pharmacology of neuronal background potassium channels. Neuropharmacology. 2003; 44:1–7. [PubMed: 12559116]

Lesage F, Guillemare E, Fink M, Duprat F, Lazdunski M, Romey G, Barhanin J. TWIK-1, a ubiquitous human weakly inward rectifying K+ channel with a novel structure. EMBO J. 1996; 15:1004–1011. [PubMed: 8605869]

Mizuno Y, Oomura Y, Hori N, Carpenter DO. Action of vasopressin on CA1 pyramidal neurons in rat hippocampal slices. Brain Res. 1984; 309:241–246. [PubMed: 6089958]

Molle M, Born J. Slow oscillations orchestrating fast oscillations and memory consolidation. Prog Brain Res. 2011; 193:93–110. [PubMed: 21854958]

Muhlethaler M, Charpak S, Dreifuss JJ. Contrasting effects of neurohypophysial peptides on pyramidal and non-pyramidal neurones in the rat hippocampus. Brain Res. 1984; 308:97–107. [PubMed: 6478205]

Muhlethaler M, Dreifuss JJ, Gahwiler BH. Vasopressin excites hippocampal neurones. Nature. 1982; 296:749–751. [PubMed: 6122162]

Raggenbass M. Overview of cellular electrophysiological actions of vasopressin. Eur J Pharmacol. 2008; 583:243–254. [PubMed: 18280467]

Raggenbass M, Goumaz M, Sermasi E, Tribollet E, Dreifuss JJ. Vasopressin generates a persistent voltage-dependent sodium current in a mammalian motoneuron. J Neurosci. 1991; 11:1609–1616. [PubMed: 1646297]

Reymond-Marron I, Tribollet E, Raggenbass M. The vasopressin-induced excitation of hypoglossal and facial motoneurons in young rats is mediated by V1a but not V1b receptors, and is independent of intracellular calcium signalling. Eur J Neurosci. 2006; 24:1565–1574. [PubMed: 17004920]

Rong XW, Chen XF, Du YC. Potentiation of synaptic transmission by neuropeptide AVP4-8 (ZNC(C)PR) in rat hippocampal slices. Neuroreport. 1993; 4:1135–1138. [PubMed: 8219041]

Somogyi P, Klausberger T. Defined types of cortical interneurone structure space and spike timing in the hippocampus. J Physiol. 2005; 562:9–26. [PubMed: 15539390]

Talley EM, Solorzano G, Lei Q, Kim D, Bayliss DA. Cns distribution of members of the two-pore-domain (KCNK) potassium channel family. J Neurosci. 2001; 21:7491–7505. [PubMed: 11567039]

Tiberiis BE, McLennan H, Wilson N. Neurohypophysial peptides and the hippocampus. II. Excitation of rat hippocampal neurones by oxytocin and vasopressin applied in vitro. Neuropeptides. 1983a; 4:73–86. [PubMed: 6669225]

Tiberiis BE, Wilson N, McLennan H. Neurohypophysial peptides and the hippocampus. I. Vasopressin immunoreactivity in the rat hippocampus. Neuropeptides. 1983b; 4:65–72. [PubMed: 6669224]

Wang S, Chen X, Kurada L, Huang Z, Lei S. Activation of group II metabotropic glutamate receptors inhibits glutamatergic transmission in the rat entorhinal cortex via reduction of glutamate release probability. Cereb Cortex. 2012; 22:584–594. [PubMed: 21677028]

Wang S, Zhang AP, Kurada L, Matsui T, Lei S. Cholecystokinin facilitates neuronal excitability in the entorhinal cortex via activation of TRPC-like channels. J Neurophysiol. 2011; 106:1515–1524. [PubMed: 21753024]

Wrobel LJ, Dupre A, Raggenbass M. Excitatory action of vasopressin in the brain of the rat: role of cAMP signaling. Neuroscience. 2011; 172:177–186. [PubMed: 20933582]

Xiao Z, Deng PY, Rojanathammanee L, Yang C, Grisanti L, Permpoonputtana K, Weinshenker D, Doze VA, Porter JE, Lei S. Noradrenergic depression of neuronal excitability in the entorhinal cortex via activation of TREK-2 K+ channels. J Biol Chem. 2009a; 284:10980–10991. [PubMed: 19244246]

Xiao Z, Deng PY, Yang C, Lei S. Modulation of GABAergic transmission by muscarinic receptors in the entorhinal cortex of juvenile rats. J Neurophysiol. 2009b; 102:659–669. [PubMed: 19494196]

Zeng W, Xu X, Muallem S. Gbetagamma transduces [Ca2+]i oscillations and Galphaq a sustained response during stimulation of pancreatic acinar cells with [Ca2+]i-mobilizing agonists. J Biol Chem. 1996; 271:18520–18526. [PubMed: 8702499]

Highlights

- We examine the effects of vasopressin on GABAergic transmission in the hippocampus
- Vasopressin increases GABA release via activation of V_{1A} receptors
- Vasopressin depolarizes GABAergic interneurons via inhibition of K^+ channels
- Vasopressin-induced depolarization is dependent on $G\alpha_{q/11}$
- Functions of PLC and PKC are not required

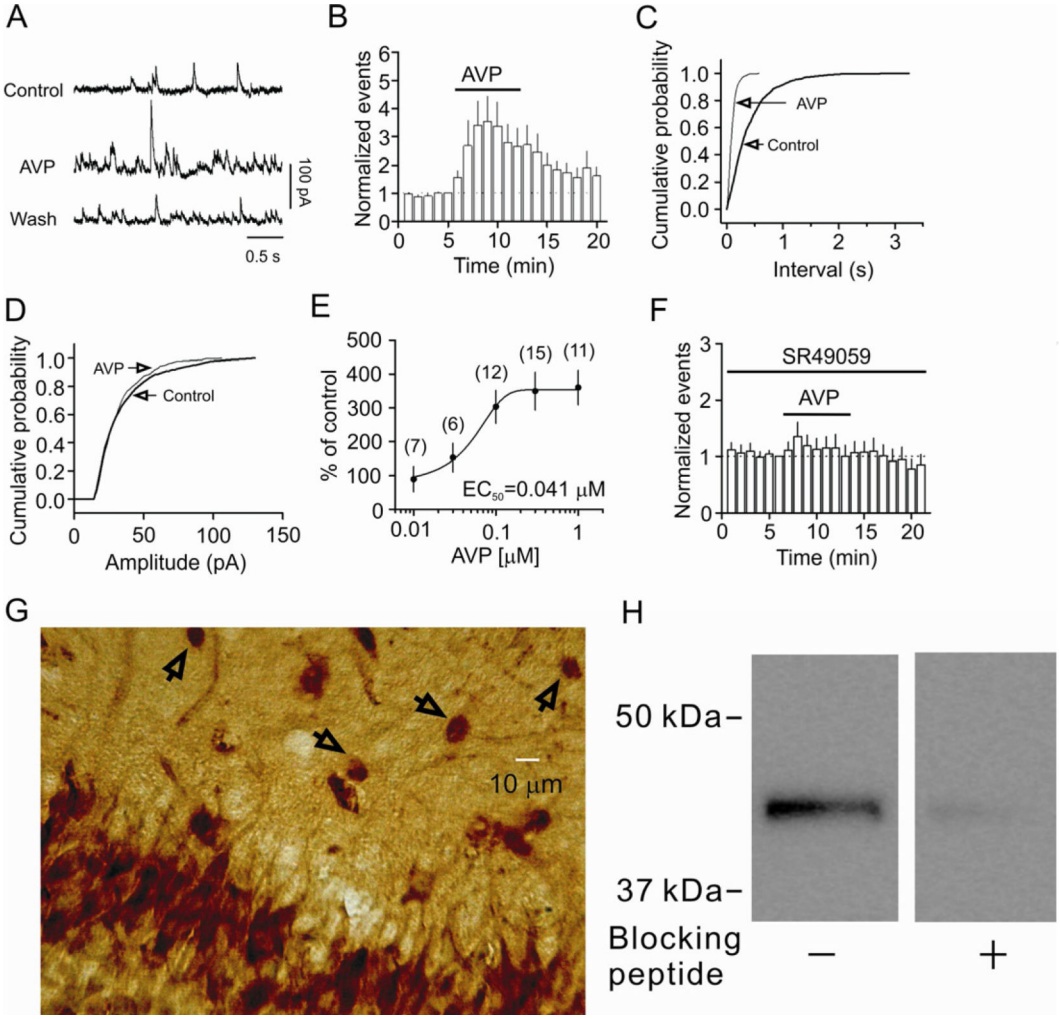

Fig. 1.

AVP increases the frequency not the amplitude of sIPSCs recorded from the CA1 pyramidal neurons of the hippocampus via activation of V_{1A} receptors. **A**, sIPSCs recorded from a CA1 pyramidal neuron before, during and after the application of AVP (0.3 μM). **B**, Time course of the sIPSC frequency averaged from 9 cells. **C**, Cumulative frequency distribution from a CA1 pyramidal neuron before and during the application of AVP. **D**, Cumulative amplitude distribution from the same cell before and during the application of AVP. **E**, Concentration-response curve of AVP. Numbers in the parenthesis are numbers of cells recorded. **F**, Pretreatment of slices with and continuous bath application of the selective V_{1A} receptor antagonist, SR49059 (1 μM), blocked AVP-induced increases in sIPSC frequency (n=8). **G**, Immunoreactivity of V_{1A} receptors was detected in both pyramidal neurons and interneurons in CA1 region. Arrows indicate interneurons in the stratum radiatum. **H**, Western blot demonstrated the expression of V_{1A} receptors in the lysates of the CA1 region. A band of ~43 kDa was detected whereas pretreatment of the V_{1A} antibody with the corresponding blocking peptide significantly reduced the density of the band demonstrating the specificity of the antibody.

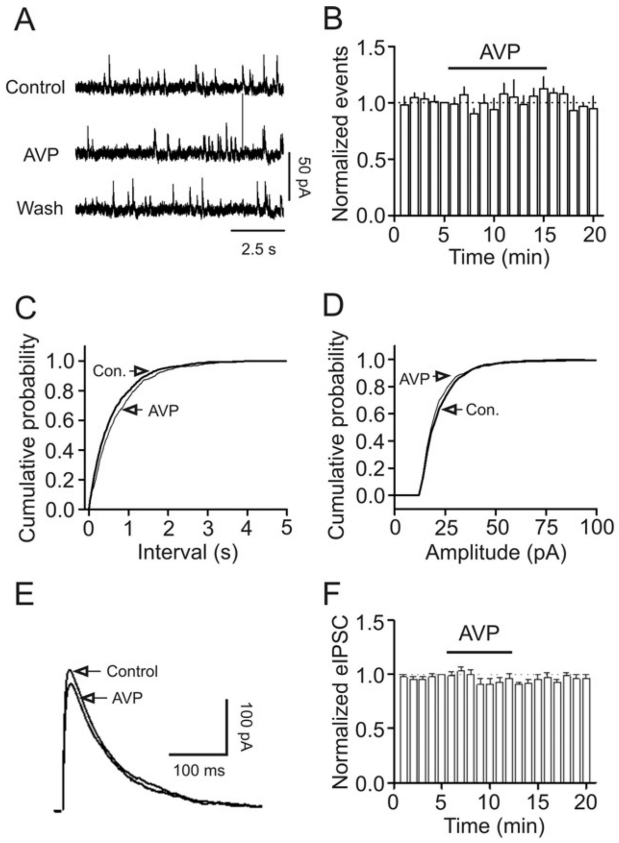

Fig. 2.

AVP does not modulate mIPSCs recorded in the presence of TTX and eIPSC recorded by placing a stimulation electrode in CA1 stratum radiatum. **A**, mIPSC current traces recorded from a CA1 pyramidal neuron before, during and after the application of AVP (0.3 μM). **B**, Time course of mIPSC frequency summarized from 5 CA1 pyramidal neurons. **C**, Cumulative frequency distribution of mIPSCs before and during the application of AVP. **D**, Cumulative amplitude distribution of mIPSCs before and during the application of AVP. Note that AVP did not change the frequency or the amplitude of mIPSCs. **E**, eIPSC traces averaged from 10 IPSCs before and during the application of AVP. **F**, Summarized time course of the eIPSC amplitude from 7 CA1 pyramidal neurons before, during and after the application of AVP (0.3 μM).

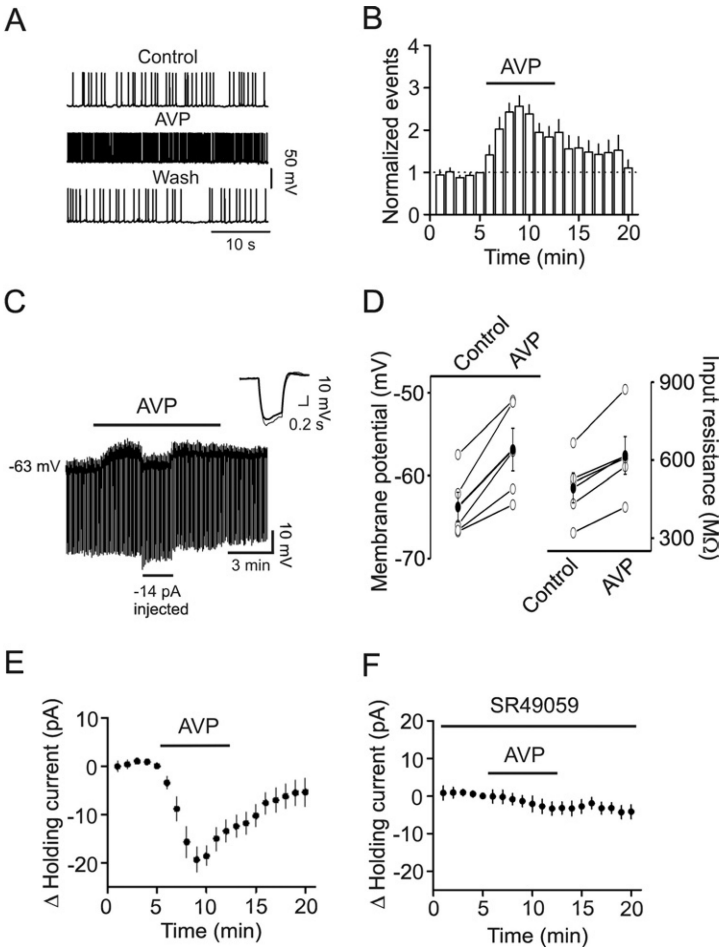

Fig. 3.

AVP increases the excitability of GABAergic interneurons in CA1 stratum radiatum. **A**, APs recorded from an interneuron before, during and after application of AVP (0.3 μM). **B**, Time course of AP firing frequency averaged from 11 interneurons. Note that AVP increased the AP firing frequency. **C**, Application of AVP (0.3 μM) generated membrane depolarization and increased input resistance in an interneuron. Resting membrane potential was recorded in current-clamp mode and a hyperpolarizing current (-50 pA, 500 ms) was injected every 5 s to measure the input resistance. Note that AVP generated depolarization and increased the input resistance. To exclude the influence of AVP-induced membrane depolarization on the input resistance, a negative current (-14 pA indicated by the horizontal bar) was injected briefly to bring the membrane potential back to the initial level. Under these conditions, the voltage responses induced by the injection of hyperpolarizing currents (-50 pA, 500 ms) were still larger compared with control suggesting that AVP-induced increases in input resistance are not secondary to its effect on membrane depolarization. Inset is the voltage traces taken before (*thick*) and during (*thin*) the application of AVP when the negative current was injected. **D**, Summarized data for AVP-induced depolarization (*left*) and increase in input resistance (*right*). Solid circles represent average values. **E**, Application of AVP (0.3 μM) induced an inward HC in interneurons. **F**, Application of SR49059 (1 μM), a V_{1A} antagonist, blocked AVP-induced increases in inward HCs.

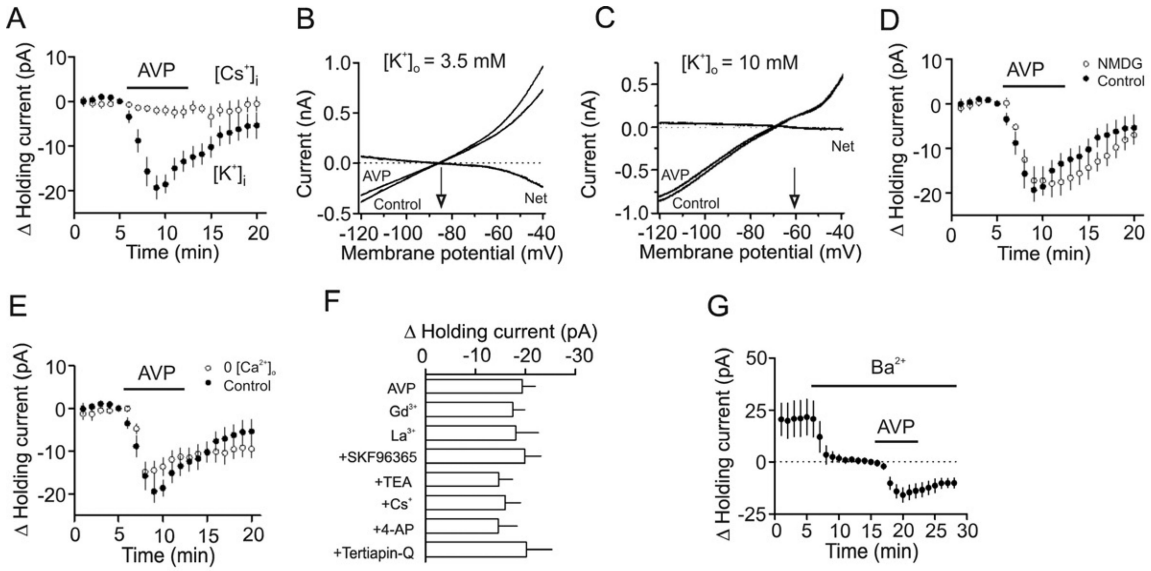

Fig. 4.

AVP-induced depolarization of interneurons is mediated by inhibition of background K^+ channels. **A**, AVP did not induce conspicuous inward HCs when the intracellular solution contained Cs-gluconate. **B**, Voltage-current relationship recorded by a ramp protocol (from -120 mV to -40 mV, at a speed of 0.07 mV/ms) in the extracellular solution containing 3.5 mM K^+ before and during the application of AVP (0.3 μM). Traces in the figure were averaged traces from 5 cells. The AVP-induced net current has a reversal potential at ~-84 mV close to the calculated K^+ reversal potential (~-85 mV). **C**, Voltage-current relationship recorded by the same ramp protocol in the extracellular solution containing 10 mM K^+ before and during the application of AVP (0.3 μM). Traces in the figure were averaged traces from 6 cells. The AVP-induced net current has a reversal potential at ~-61 mV close to the calculated K^+ reversal potential (~-58.7 mV). **D**, Replacement of extracellular NaCl with NMDG-Cl failed to change AVP-mediated increases in inward HCs significantly. **E**, Bath application of AVP (0.3 μM) still induced a comparable inward HC in the extracellular solution containing 0 Ca^{2+}. **F**, Inclusion of Gd^{3+} (10 μM), La^{3+} (10 μM) or SKF96365 (100 μM) in the extracellular solution had no effects on AVP-induced increases in inward HCs. Similarly, inclusion of the classical K^+ channel blockers (TEA, Cs^+, 4-AP, tertiapin-Q) in the extracellular solution did not significantly alter AVP-mediated increases in inward HCs. **G**, Bath application of Ba^{2+} (2 mM) induced an inward HC by itself but did not block AVP-induced increases in inward HCs.

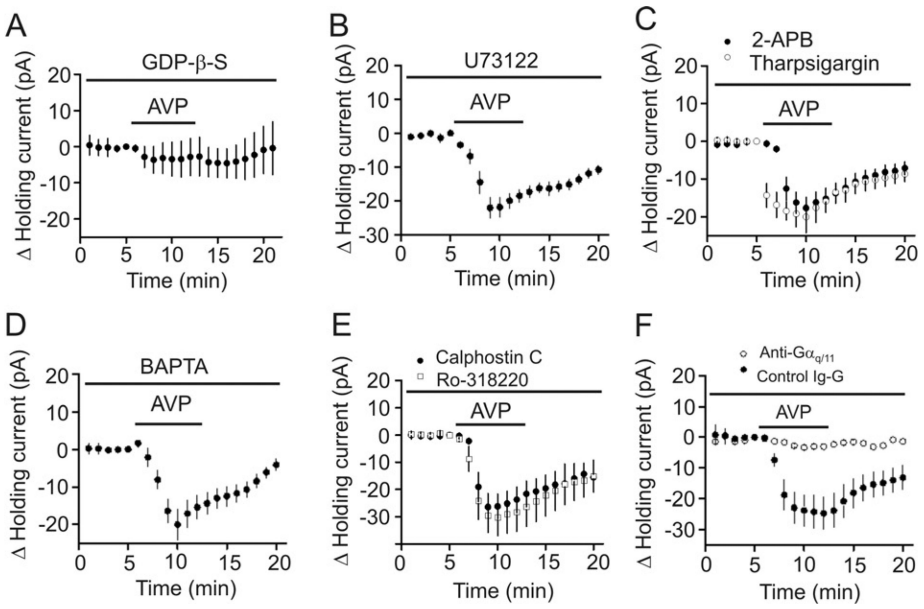

Fig. 5.

AVP-induced depolarization of hippocampal interneurons is dependent on G$\alpha_{q/11}$ but independent of PLC, intracellular Ca^{2+} release and PKC. **A**, Inclusion of GDP-β-S (2 mM) in the recording pipettes blocked the effects of AVP on HCs. **B**, Pretreatment of slices with and continuous bath application of U73122 (10 μM) did not change AVP-induced increases in inward HCs. **C**, Pretreatment of slices with and continuous bath perfusion of 2-APB (100 μM) or intracellular application of tharpsigargin (10 μM) via the recording pipettes had no significant effects on AVP-induced increases in inward HCs. **D**, Intracellular perfusion of BAPTA (10 mM) via the recording pipettes had no significant effects on AVP-mediated increases in inward HCs. **E**, Pretreatment of slices with and continuous bath perfusion of calphostin C (1 μM) and Ro-318220 (1 μM) did not change AVP-induced increases in inward HCs significantly. **F**, Intracellular dialysis of anti-G$\alpha_{q/11}$ antibody via the recording pipettes significantly reduced AVP-mediated increases in inward HCs but intracellular application of the control Ig-G did not alter AVP-induced increases in inward HCs.

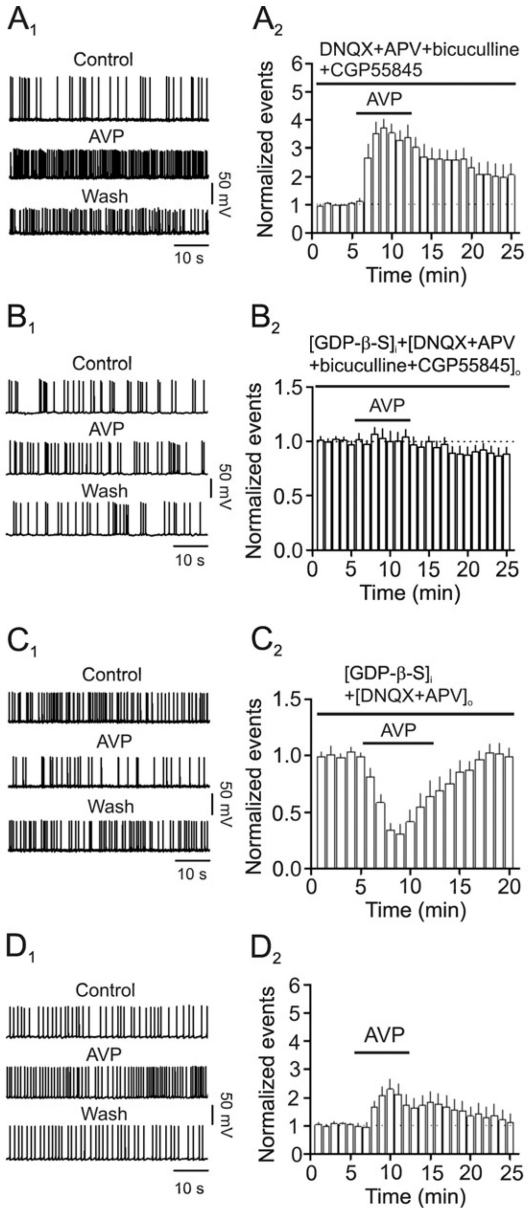

Fig. 6.

Effects of AVP on the excitability of CA1 pyramidal neurons in distinct conditions. **A_1-A_2**, Bath application of AVP (0.3 μM) increased the firing frequency of APs recorded from CA1 pyramidal neurons in the extracellular solution containing DNQX (10 μM), *dl*-APV (100 μM), bicuculline (10 μM) and CGP55845 (2 μM). **A_1**, APs recorded from a CA1 pyramidal neuron before, during and after the application of AVP. **A_2**, Summarized data from 8 cells. **B_1-B_2**, Bath application of AVP (0.3 μM) did not significantly increase the firing frequency of APs recorded from CA1 pyramidal neurons in the extracellular solution containing DNQX (10 μM), *dl*-APV (100 μM), bicuculline (10 μM) and CGP55845 (2 μM) and intracellular solution containing GDP-β-S (2 mM). **B_1**, APs recorded from a CA1 pyramidal neuron before, during and after the application of AVP. **B_2**, Summarized data from 8 cells. **C_1-C_2**, Bath application of AVP (0.3 μM) transiently decreased the firing frequency of APs recorded from CA1 pyramidal neurons in the extracellular solution containing DNQX (10 μM) and *dl*-APV (100 μM) and intracellular solution containing GDP-β-S (2 mM). **C_1**, APs

recorded from a CA1 pyramidal neuron before, during and after the application of AVP. **C_2**, Summarized data from 7 cells. **D_1-D_2**, Bath application of AVP (0.3 μM) increased the firing frequency of APs recorded from CA1 pyramidal neurons in normal extracellular and intracellular solution. **D_1**, APs recorded from a CA1 pyramidal neuron before, during and after the application of AVP. **D_2**, Summarized data from 7 cells.